

INTRODUCTION

The High Luminosity upgrade of the Large Hadron Collider will increase the integrated luminosity by about a factor of 5. To cope with the higher muon flux rate, and the subsequently higher L1A trigger rate, the Phase-2 Muon system upgrade is underway [1]. One of the detectors proposed for the upgrade is the ME0 triple-Gas Electron Multiplier (GEM) detector, which will increase coverage between $2.0 < |\eta| < 2.8$ (see Fig. 1) and consequently help control the level 1 trigger rate.

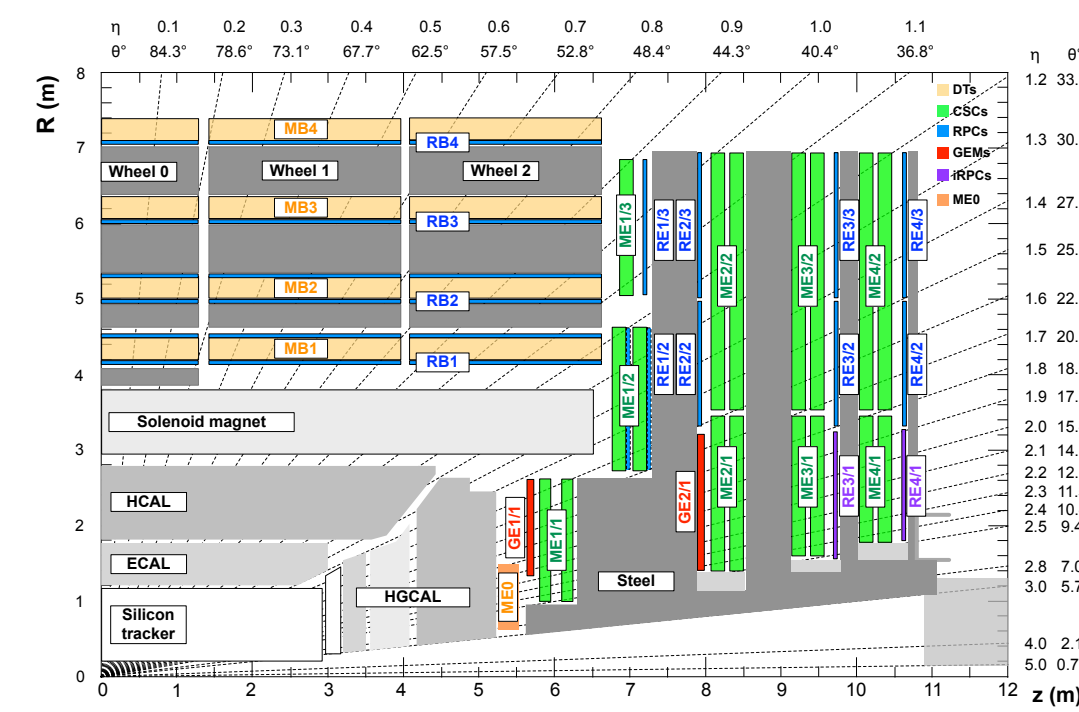


Figure 1: Quadrant of the upgraded CMS experiment with the ME0 in orange [1].

This detector differs from previous CMS GEM detectors in that it features high voltage (HV) segmentation with protection resistors on both sides of

the foil (i.e., the foils are double-segmented) to help protect from HV discharges. During the quality control tests on a prototype ME0 detector, distinct signals were observed in sectors other than those being irradiated. This crosstalk poses a significant problem for the operation of these chambers in the experiment, and must be mitigated before full-scale production begins. This poster discusses the characterization and mitigation of the crosstalk in this detector, as well as the impact this crosstalk has on detector performance.

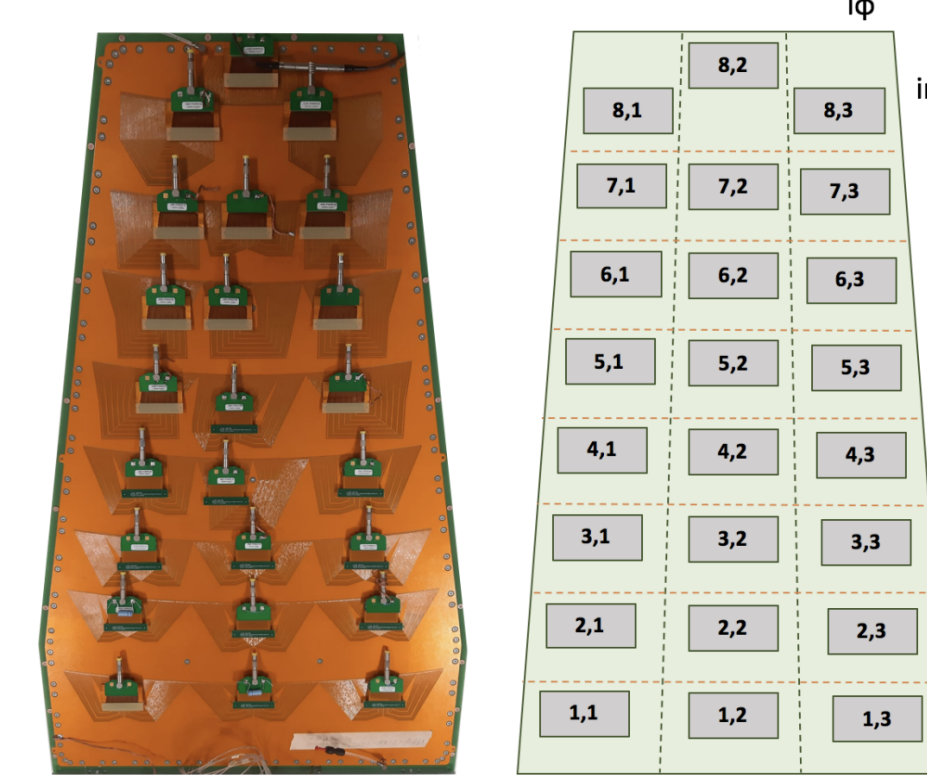


Figure 2: The ME0 and its readout sector mapping.

CHARACTERIZATION OF CROSTALK

The pulses read out from a GEM detector under normal operation are approximately square pulses of 10 ns width. To investigate the nature of the crosstalk, we used signal generators to apply square voltage pulses with 1 μ s widths to all 128 strips in one readout (RO) sector. Ideally, pulse widths of ~ 10 ns would have been used, but with the capabilities of the signal generator used, square pulses under 1 μ s became severely distorted due to an impedance mismatch. Thus, we used a one microsecond pulse width for these studies. To measure and quantify the crosstalk, oscilloscope traces were recorded and then manually measured (see Fig. 3 for a representative example).

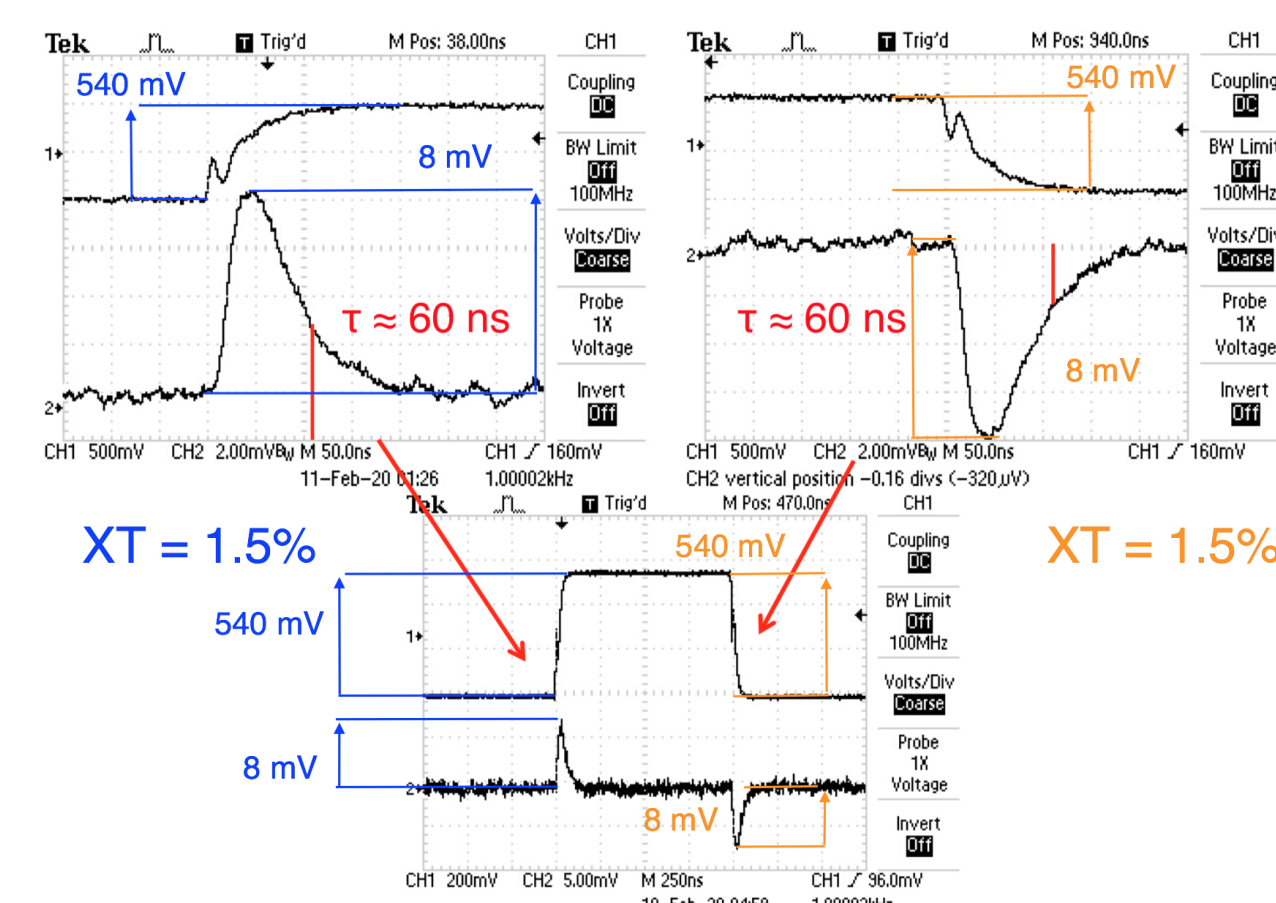


Figure 3: Some example oscilloscope traces of the input square pulse (ch. 1, top) and the crosstalk signal (ch. 2, bottom).

The crosstalk percentage is quantified as the ratio of output pulse amplitude to the input amplitude, with error given by the standard error propagation formula below.

$$XT\% = \frac{V_{out}}{V_{in}} \cdot 100\%$$

$$\delta(XT\%) = |XT\%| \sqrt{\left(\frac{\delta V_{in}}{V_{in}}\right)^2 + \left(\frac{\delta V_{out}}{V_{out}}\right)^2} \cdot 100\%$$

Comprehensive crosstalk “maps” (see an example in Fig. 4) were made by reading out the signal in all of the other readout (RO) sectors in the chamber. These maps place an upper limit on the crosstalk and the extent to which neighboring sectors in the chamber are affected. The range of the average observed crosstalk are listed in Tab. 1.

The crosstalk signal is a result of CR differentiation: the capacitive coupling between RO sectors (and interstrip capacitance) forms the capacitor (average measured intersector capacitance $C = 702 \pm 18$ pF), and the resistance of the cable (50Ω) used to read out the signal serves as the resistor. The time constant is then $\tau \approx 35$ ns. This hypothesis was verified by examining the time constant of the crosstalk pulses and also by varying the input square pulse widths T , which shows the characteristic behavior of a CR differentiator as the pulse width $T \gg \tau$ and $T \approx \tau$ (see Fig. 5). These results are also verified via simulation in a complementary talk by M. Hohlmann, see [2].

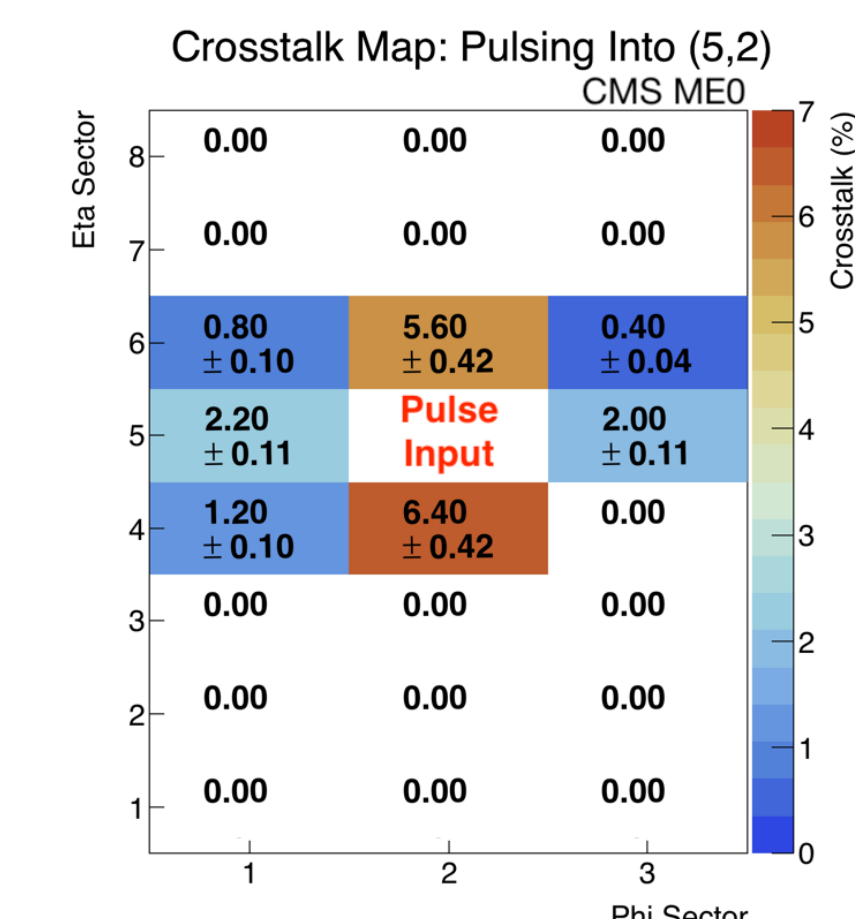


Figure 4: An example crosstalk map with pulse input in (5,2). Note the symmetric behavior in adjacent $i\phi$ partitions (and $i\eta$ partitions). Sectors with $XT = 0.0\%$ showed no discernible crosstalk.

$i\eta$ Sector	Minimum Crosstalk (%)	Maximum Crosstalk (%)
1	0.24 ± 0.04	3.80 ± 0.21
5	0.20 ± 0.04	6.40 ± 0.42
8	0.16 ± 0.04	4.00 ± 0.22

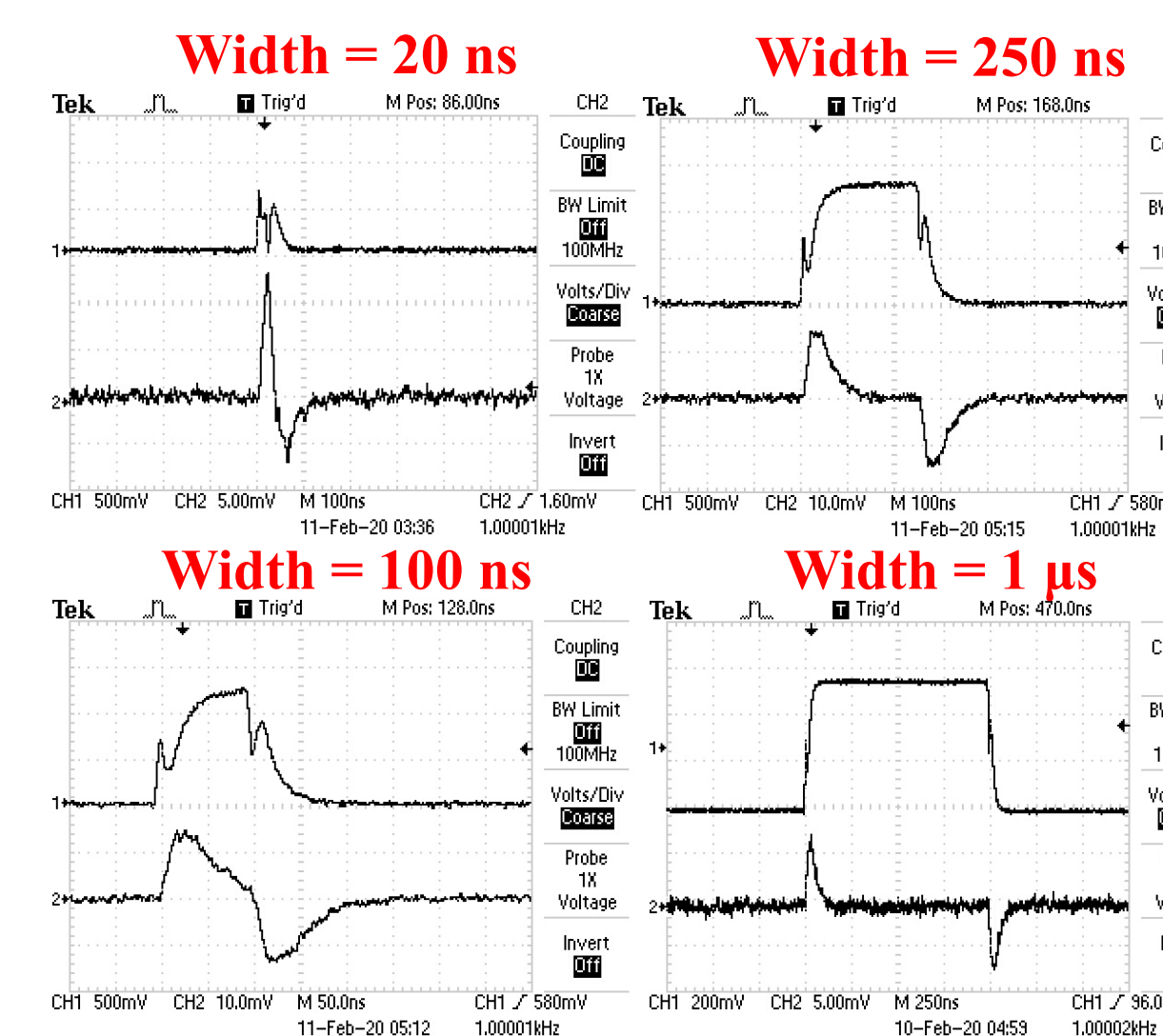


Figure 5: Crosstalk pulse shapes with different input square pulse widths. Note that below 1 μ s, the input pulses were distorted due to impedance mismatch.

IMPACT ON DETECTOR PERFORMANCE

To understand the impact that the crosstalk has on detector performance, we performed dead time, timing error, and efficiency simulations. Experimental results of determining the probability of observing a crosstalk pulse were used as input parameters to a simulation of the background rate. To determine the crosstalk probability, a GE1/1 GEM detector with double-segmented foils was irradiated with alpha and beta sources through a small hole in the GEM drift cathode PCB, and the hit rate of the pulses above threshold were recorded. Dead time and timing error simulations of the frontend ASIC hybrid cards were performed by injecting a signal pulse at a fixed time into the simulated shaping circuit, and then varying the injection time of a crosstalk pulse into the same, simulated circuit of the ASIC. It was discovered that a maximum timing error of about 550 ns result from the interference of the crosstalk signal. Results of background particle rate simulation in CMS were used in tandem with the dead time simulations to determine the loss of efficiency of the detector. Figure 6 displays the results of these studies, which shows the nominal detector efficiency and the effi-

ciency loss from the dead time due to crosstalk, for each readout partition ($i\eta$ number) in the detector.

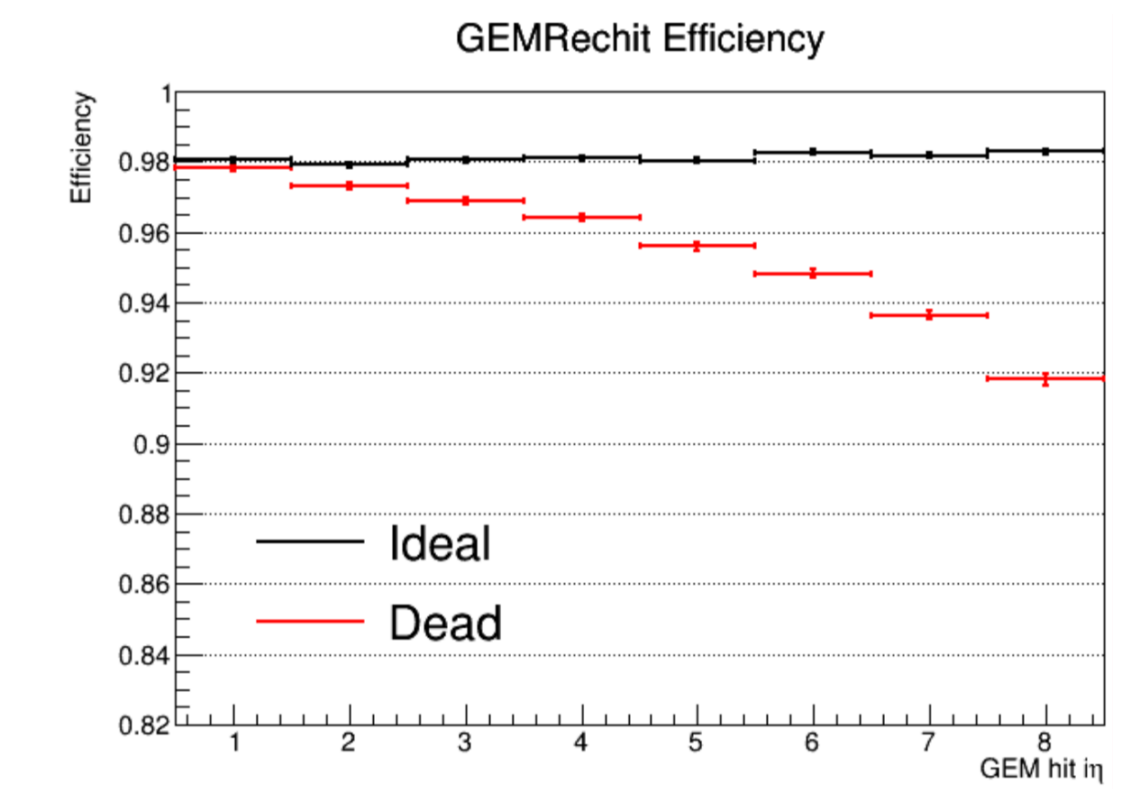


Figure 6: Plot of the reconstructed efficiencies and the losses due to crosstalk. (With a dead time of 50 bunch crossings.)

MITIGATION STRATEGIES

Several mitigation strategies were employed to ameliorate the crosstalk: increasing the area of the HV segments on the bottom of the foil, both with and without a low-pass filter, and including 5 bypass capacitors in one $i\eta$ segment. For the first study, we soldered five, 330 pF bypass capacitors in parallel to the HV segments $i\eta = 8$, and removed the protection resistors in $i\eta = 5$ and then connected the HV segments in parallel to increase the capacitance of the third GEM foil (see Fig. 7). Crosstalk maps were then taken for pulse inputs into each RO connector in $i\eta = 5, 8$. We then repeated crosstalk measurements for all of the HV segments on the bottom of third GEM foil connected in parallel with solder, both with a low-pass circuit and both without the HV divider.

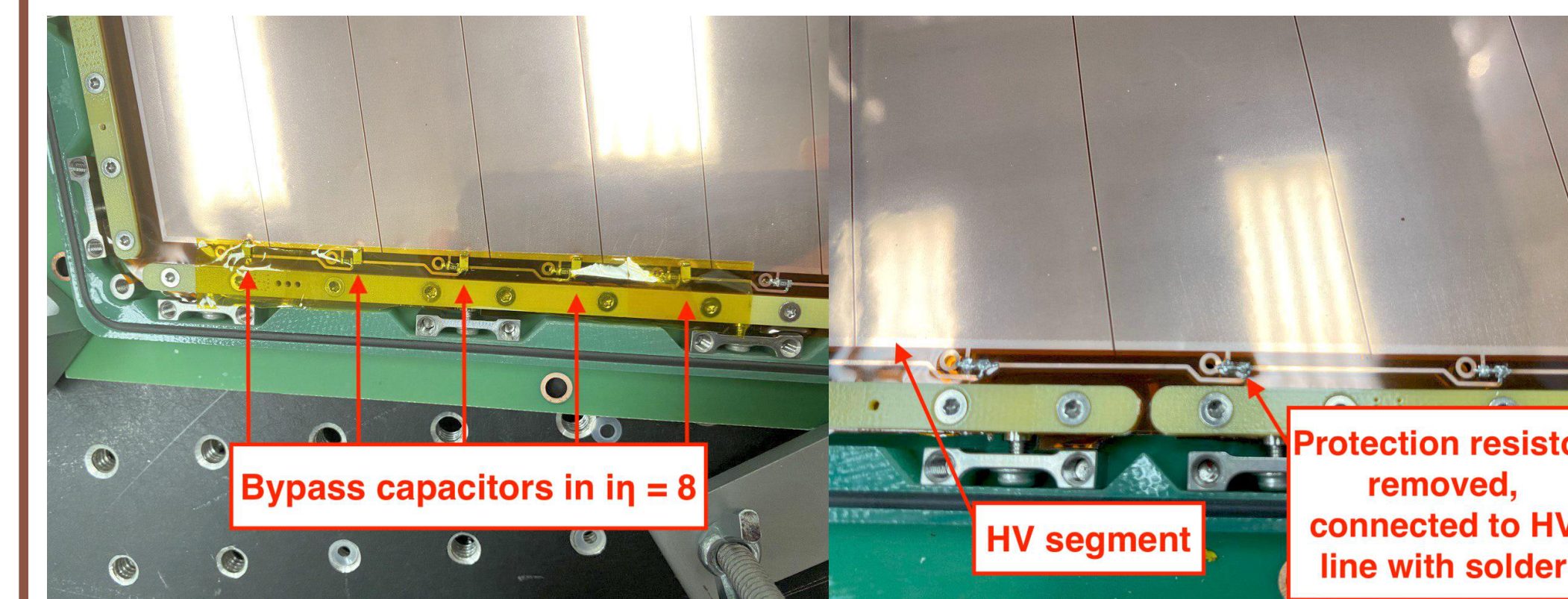


Figure 7: Image of the modifications on the bottom of the third GEM foil.

The results, quoted as a change in percentage are listed in Tab. 2 below. For a summary of all mitigation strategies when pulsing into sector (5,2), see Fig. 8. It should be noted that a negligibly small value of crosstalk ($\approx 0.4\%$) was observed in all $i\phi$ partitions in all $i\eta$ sectors after these modifications were made. Overall, the average observed crosstalk is reduced by each mitigation strategy, with the largest decrease in crosstalk occurring when the third GEM foil is single-segmented (i.e., protection resistors on the top-side of the foil, only), with the HV divider and low-pass filter.

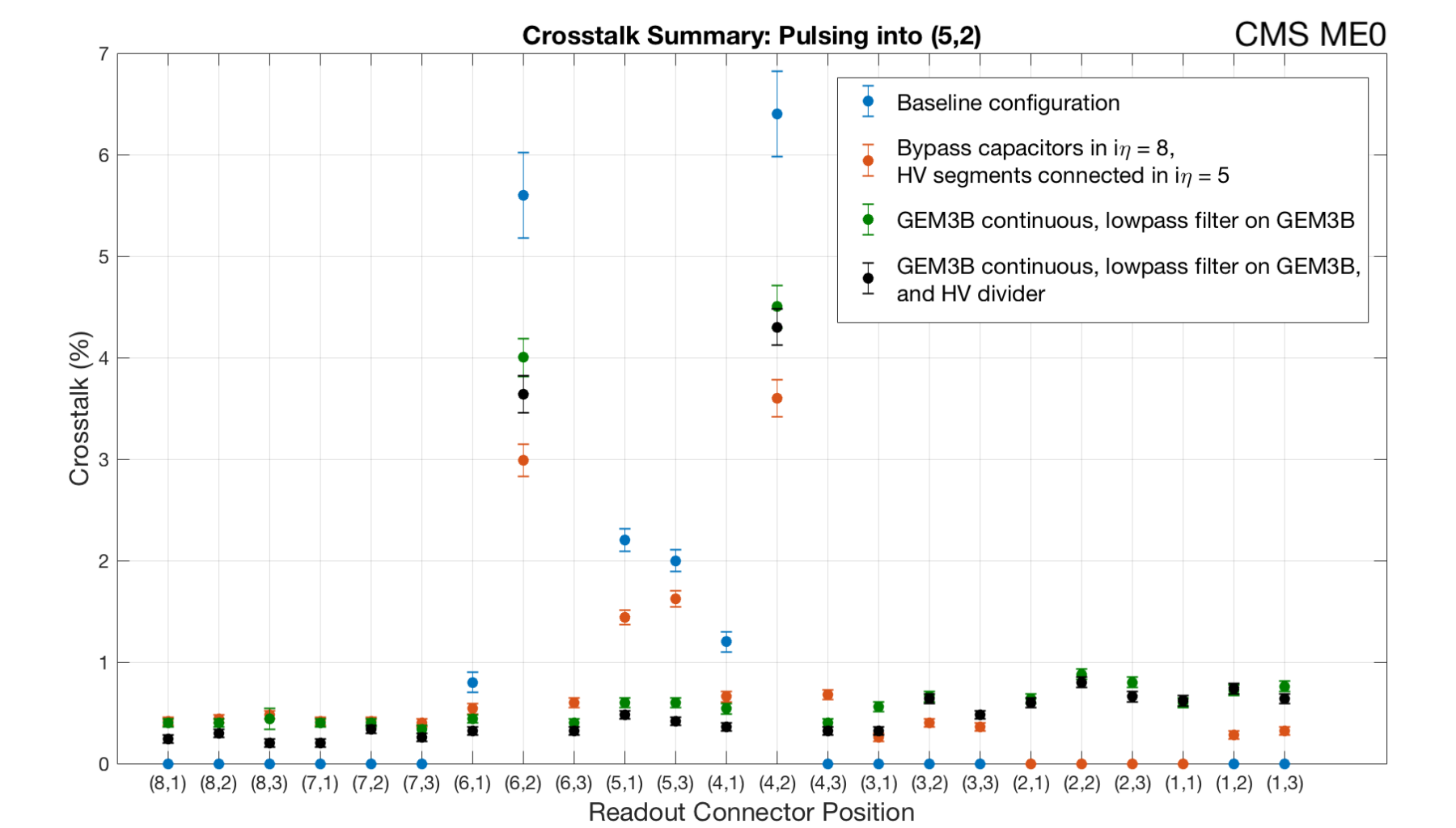


Figure 8: Summary plot of the crosstalk in all sectors with pulse input into (5,2).

Pulsing into	Bypass Cap. & HV segments connected in $i\eta = 5$	GEM3B Continuous, HV Filter (w/o Divider)	GEM3B Continuous, HV Filter (w/Divider)
$i\eta = 8$	$-0.47 \pm 0.04\%$	$-0.50 \pm 0.04\%$	$-0.53 \pm 0.03\%$
$i\eta = 5$	$+0.03 \pm 0.04\%$	$-0.05 \pm 0.05\%$	$-0.36 \pm 0.07\%$
$i\eta = 1$	N/A	$-0.17 \pm 0.04\%$	$-0.39 \pm 0.05\%$
Grand Average	$-0.22 \pm 0.03\%$	$-0.24 \pm 0.03\%$	$-0.43 \pm 0.03\%$

SUMMARY AND CONCLUSION

In general, crosstalk is seen in all $i\phi$ partitions of a readout sector that is being pulsed, with crosstalk extending to the nearest neighboring $i\eta$ segments in the CMS ME0 GEM detector with double-segmented foils. This crosstalk is due to the capacitive coupling between RO sectors. We see that while a small value of crosstalk is introduced into other RO sectors by modifying the foil, the crosstalk is successfully reduced, with a maximum average reduction of $-0.43 \pm 0.03\%$ where the bottom of the third GEM foil is continuous (single-segmentation) and has a low-pass filter and HV divider. Simulations indicate that without these modifications, there would be a maximum efficiency loss of $\sim 6\%$.

ACKNOWLEDGEMENTS

We would like to thank the U.S. DOE (HEP) and the NSF (Cornell University subaward, P.I. Dr. Marcus Hohlmann), for their support of this work, and all members of the CMS GEM group for their contributions to this project.

REFERENCES

- [1] CMS Collaboration, *The Phase-2 Upgrade of the CMS Muon Detectors Technical Design Report*, CERN-LHCC-2017-012, CMS-TDR-016, Sep. 12, 2017. Available: <https://cds.cern.ch/record/2293189?ln=en>.
- [2] M. Hohlmann, “A MODEL FOR CROSTALK IN MICRO-PATTERN GAS DETECTORS,” poster N-30-150 presented at IEEE NSS-MIC 2020, Nov. 2, 2020.